



HAL
open science

Functional analysis of AtlA, the major N-acetylglucosaminidase of *Enterococcus faecalis*.

Catherine Eckert, Maxime Lecerf, Lionel Dubost, Michel Arthur, Stéphane
Mesnage

► **To cite this version:**

Catherine Eckert, Maxime Lecerf, Lionel Dubost, Michel Arthur, Stéphane Mesnage. Functional analysis of AtlA, the major N-acetylglucosaminidase of *Enterococcus faecalis*.. *Journal of Bacteriology*, 2006, 188 (24), pp.8513-9. 10.1128/JB.01145-06 . inserm-00156004

HAL Id: inserm-00156004

<https://inserm.hal.science/inserm-00156004>

Submitted on 19 Jun 2007

HAL is a multi-disciplinary open access archive for the deposit and dissemination of scientific research documents, whether they are published or not. The documents may come from teaching and research institutions in France or abroad, or from public or private research centers.

L'archive ouverte pluridisciplinaire **HAL**, est destinée au dépôt et à la diffusion de documents scientifiques de niveau recherche, publiés ou non, émanant des établissements d'enseignement et de recherche français ou étrangers, des laboratoires publics ou privés.

ABSTRACT

21
22 The major peptidoglycan hydrolase of *E. faecalis*, AtlA, has been identified but its enzyme
23 activity remains unknown. We have used tandem mass spectrometry analysis of peptidoglycan
24 hydrolysis products obtained using the purified protein to show that AtlA is an *N*-
25 acetylglucosaminidase. To gain insight into the regulation of its enzyme activity, the three
26 domains of AtlA were purified alone or in combination following expression of truncated forms
27 of the *atlA* gene in *E. coli* or partial digestion of AtlA by proteinase K. The central domain of
28 AtlA was catalytically active, but its activity was more than two orders of magnitude lower than
29 that of the complete protein. Partial proteolysis of AtlA was detected *in vivo*: zymograms of *E.*
30 *faecalis* extracts revealed two catalytically active protein bands of 62 and 72 kDa that were both
31 absent in extracts from an *atlA* null mutant. Limited digestion of AtlA by proteinase K *in vitro*
32 suggested that the proteolytic cleavage of AtlA in *E. faecalis* extracts corresponds to the
33 truncation of the N-terminal domain, which is rich in threonine and glutamic acid residues. We
34 show that the truncation of the N-terminal domain from recombinant AtlA has no impact on
35 enzyme activity. The C-terminal domain of the protein, which contains six LysM modules bound
36 to highly purified peptidoglycan, was required for optimal enzyme activity. These data indicate
37 that AtlA is not produced as a proenzyme and that control of the AtlA glucosaminidase activity is
38 likely to occur at the level of LysM-mediated binding to peptidoglycan.

INTRODUCTION

39
40 Peptidoglycan (or murein) is a major component of the bacterial cell wall. This molecule
41 forms a bag-shaped exoskeleton enclosing the plasma membrane and protects the cell against
42 internal osmotic pressure in hypo-osmotic conditions (23). Peptidoglycan consists of glycan
43 strands of alternating β -1,4-linked *N*-acetylglucosamine (GlcNAc) and *N*-acetylmuramic acid
44 (MurNAc) residues cross-linked to each other by short peptides made of L- and D-amino acids
45 (20). Throughout growth, the insertion of new precursors and separation of daughter cells
46 requires limited cleavage of the peptidoglycan molecule (13). The enzymes responsible for this
47 process are potentially lethal enzymes referred to as autolysins as they cleave the high molecular
48 weight polymer. In addition to their contribution to cell growth and division, some autolysins
49 play a role in adhesion (8, 17) and in amplification of the inflammatory response by releasing
50 muramyl-peptides (6). Depending on the bond they cleave, autolysins are classified as lytic
51 transglycosylases, *N*-acetylmuramidases, *N*-acetylglucosaminidases, *N*-acetylmuramoyl L-alanine
52 amidases, or endopeptidases.

53 In *Enterococcus faecalis*, two autolytic activities have been described (12). One of the
54 corresponding proteins, designated AtlA in this report, has been identified (4, 18) but its activity
55 has not been characterized. AtlA is a three-domain enzyme composed of an N-terminal
56 threonine- and glutamic acid-rich (T/E-rich) domain of unknown function (domain I), a central
57 putative catalytic domain (domain II) and a C-terminal cell wall binding domain consisting of six
58 LysM modules (domain III) (3). In this study, we have identified the peptidoglycan bond cleaved
59 by AtlA and analyzed the contribution of the domains of the protein to its enzyme activity.

MATERIALS AND METHODS

60

61 **Bacterial strains, plasmids, and growth conditions.** All strains and plasmids used in this
62 study are described in Table 1. The bacteria were grown at 37°C in Brain Heart Infusion broth or
63 agar (15 g/l) (BHI, Difco laboratories, Detroit, USA). When required, the growth medium was
64 supplemented with 100 µg/ml ampicillin and 50 µg/ml kanamycin.

65 **Plasmid construction.** To construct pML118 encoding amino acids 54 to 737 of AtIA
66 (domains I-II-III), V583 genomic DNA (19) was PCR-amplified using Vent DNA polymerase
67 (Biolabs) and oligonucleotides EF0799-1 and EF0799-4 (Table 1). The resulting fragment was
68 cloned in frame with the hexahistidine sequence of pET2818, a pET2816b derivative (9), using
69 NcoI and BamHI. The same cloning procedure was used to obtain pML318 (encoding domains I-
70 II of AtIA, amino acids 54 to 335) with primers EF0799-1 and EF0799-2; pML418 (encoding
71 domain II, amino acids 182 to 335) with EF0799-3 and EF0799-2; and pML518 (encoding
72 domain III, amino acids 335 to 737) with EF0799-5 and EF0799-4.

73 **Production and purification of histidine-tagged AtIA and its derivatives.** *E. coli* BL21
74 DE3 (pREP4GroESL) (1) harboring recombinant plasmids were grown at 37°C in BHI broth
75 containing kanamycin and ampicillin. When the cultures had reached an optical density at 600
76 nm of 0.7, production of the recombinant protein was induced by addition of 0.5 mM isopropyl-
77 β-D-thiogalactopyranoside (IPTG) and incubation was continued for 12 h at 16°C. The cells were
78 harvested, washed, and resuspended in buffer A (50 mM Tris-HCl, pH 7.5, 300 mM NaCl).
79 Crude lysates were obtained by sonication (6 times 30 sec, 20 % output, Branson Sonifier 450).
80 Proteins were loaded onto Ni²⁺-nitrilotriacetate agarose resin (Qiagen GmbH, Hilden, Germany)
81 and eluted with stepwise increasing concentrations of imidazole (25, 50, 100, and 250 mM in
82 buffer A). AtIA eluting at 100 mM imidazole was further purified by anion exchange

83 chromatography (MonoQ column, Amersham biosciences, Uppsala, Sweden) using a 0 to 1 M
84 NaCl gradient in 25 mM ethanolamine (pH 9.25). The concentration of purified proteins was
85 determined using the BIO-RAD Protein Assay (BIO-RAD Laboratories GmbH, Postfach,
86 Germany).

87 AtIA derivatives were purified by the same method except that a single affinity
88 chromatography step was carried out.

89 **Proteolysis of AtIA.** Purified AtIA (10 µg) was incubated with 10 ng of proteinase K
90 (Boehringer GmbH, Ingelheim, Germany) in 20 µl of 25 mM Tris-HCl, pH 7.5, 25 mM NaCl,
91 0.5 mM MgCl₂, and 2 mM CaCl₂ (buffer B). After various incubation times at 37°C (1 to 10
92 min), aliquots were withdrawn and digestion was stopped by adding phenylmethylsulfonyl
93 fluoride to a final concentration of 2 mM. The samples were analyzed by SDS-PAGE. For N-
94 terminal sequencing, proteins were transferred onto polyvinylidene difluoride membranes by
95 passive absorption and sequenced using a Perkin-Elmer Procise 494 HT protein sequencer as
96 described elsewhere (10).

97 To prepare AtIA with a truncated domain I, 400 µg of purified protein were digested with 12.5
98 ng of proteinase K for 3 h at 37°C in 500 µl of buffer B. The digestion products were separated
99 by size exclusion chromatography on a Superdex75 HR 10/30 column (Amersham biosciences,
100 Uppsala, Sweden) equilibrated with 20 mM Tris-HCl, pH 7.5, 100 mM NaCl. The fractions
101 containing undigested AtIA and partially digested AtIA were analyzed by SDS-PAGE, pooled
102 separately, and tested for activity.

103 **Cell wall purification and peptidoglycan structural analysis.** Bacteria were grown in 500 ml
104 of BHI broth at 37 °C to an optical density at 650 nm of 0.7. Peptidoglycan was extracted by
105 treating the bacterial pellet with 14 ml of 4% SDS at 100 °C for 30 min. Peptidoglycan was
106 washed five times by centrifugation (12,000 x g for 10 min at 20 °C) with 20 ml of water.

107 Peptidoglycan was serially treated overnight at 37 °C with Pronase (200 µg/ml) in 1 ml of Tris-
108 HCl (10 mM, pH 7.4) and with trypsin (200 µg/ml) in 1 ml of phosphate buffer (20 mM, pH 7.8).
109 Peptidoglycan was washed twice with 20 ml of water and digested overnight with mutanolysin
110 (45 µg/ml; Sigma-Aldrich) or AtIA(200 µg/ml) at 37 °C in 1 ml of phosphate buffer (25 mM,
111 pH 6.0) containing MgCl₂ (0.1 mM). soluble disaccharide peptides were recovered by
112 ultracentrifugation (100,000 x g for 30 min at 20 °C). For reduction of MurNAc to *N*-
113 acetylmuramitol or GlcNAc to *N*-acetylglucosaminitol, equal volumes (200 µl) of the solution of
114 disaccharide peptides and of borate buffer (250 mM, pH 9.0) were mixed. Two mg of sodium
115 borohydride were added, and the solution was incubated for 20 min at room temperature. The pH
116 of the solution was adjusted to 4.0 with 20% orthophosphoric acid.

117 The reduced muropeptides were separated by reverse-phase high-performance liquid
118 chromatography (rp-HPLC) on a C₁₈ column (3 µm, 4.6 by 250 mm; Interchrom, Montluçon,
119 France) at a flow rate of 0.5 ml/min with a 0 to 20 % gradient applied between 10 and 90 min
120 (buffer A, 0.05 % [vol/vol] trifluoroacetic acid in water; buffer B, 0.035 % [vol/vol]
121 trifluoroacetic acid in acetonitrile). Mass spectral data were collected with an electrospray time-
122 of-flight mass spectrometer operating in the positive mode (Qstar Pulsar I; Applied Biosystems,
123 Courtaboeuf, France). The data were acquired with a capillary voltage of 5,200 V and a
124 declustering potential of 20 V. The mass scan range was from *m/z* 350 to 1,500, and the scan
125 cycle was 1s. Tandem mass spectrometry was carried out as previously described (2).

126 **Determination of peptidoglycan hydrolase activity.** Hydrolysis of purified cell walls
127 (200 µg/ml) was measured using an Ultrospec 2000 spectrophotometer (Amersham biosciences,
128 Uppsala, Sweden) and following the decrease in turbidity at 450 nm for 1 h at 37°C in 25 mM
129 Tris-HCl, pH 7.5, 100 mM NaCl buffer. Various dilutions of AtIA and its derivatives were tested

130 to identify conditions in which the velocity of hydrolysis was proportional to enzyme
131 concentration. Enzymatic activity was expressed as A₄₅₀ units per min per mmol of protein.

132 To determine the optimal pH for AtlA activity, a buffer containing 30 mM malonic acid,
133 30 mM sodium phosphate, 30 mM Tris-HCl, and 30 mM ethanolamine was prepared and the pH
134 adjusted as required.

135 To determine whether partial proteolysis stimulated AtlA activity, 25 ng of proteinase K was
136 added to the reaction mixture containing 1 µg of AtlA in a final volume of 1 ml. In these
137 experiments, aliquots were analyzed by SDS-PAGE to monitor partial digestion of AtlA.

138 For zymogram analysis, crude extracts were separated by SDS-PAGE using gels containing
139 0.2 % autoclaved *Micrococcus lysodeikticus* cells. After electrophoresis, the proteins were
140 renatured by incubating the gel for 24 h in 25 mM Tris (pH 8.0) buffer containing 0.1 % Triton at
141 37°C. Lytic activities could be visualized as clear bands on the opaque SDS-PAGE gel.

142 **Analysis of the LysM-peptidoglycan interaction.** Purified peptidoglycan (100 µg) was
143 incubated with purified LysM domain III (10 µg) in 20 mM Tris-HCl (pH 8.0), 500 mM NaCl in
144 a final volume of 125 µl for 30 min at 4°C under agitation. The suspension was centrifuged for
145 10 min at 15,000 g and the supernatant (soluble fraction) was kept for further analyses. The pellet
146 was washed twice with 250 µl of buffer and resuspended in 125 µl of buffer (insoluble fraction).
147 Unbound proteins in the soluble fractions and bound proteins in the insoluble fractions were
148 analyzed by 12% SDS-PAGE.

RESULTS AND DISCUSSION

Enzymatic activity and purification of recombinant AtlA. Mature AtlA (residues 54 to 737, EF0799 at www.tigr.org or ALYS_ENTFA, accession P37710 in Swissprot) was produced in *E. coli* as a C-terminally histidine-tagged protein and purified using affinity and anion exchange chromatography (Fig. 1A). The purified recombinant protein migrated as a 72 kDa polypeptide band on SDS-PAGE in agreement with the predicted molecular mass of 72,540 kDa. A faint polypeptide band of approximately 62 kDa was present in all the purification steps (data not shown). Storage of the recombinant enzyme at 4°C for eight weeks led to an increase in the abundance of this 62 kDa polypeptide, indicating that it resulted from proteolysis (data not shown).

The optimal pH for the activity of recombinant AtlA was 7.0 at 37°C (Fig. 1B). Pre-incubation of the enzyme (at a concentration of 15 nM) in 10 mM EDTA did not inhibit its activity indicating that divalent cations are not essential for AtlA activity. AtlA was more active on *M. lysodeikticus* (1,900 ± 290 U), a reference substrate for autolysins, than on *E. faecalis* peptidoglycan (350 ± 20 U). The fact that *M. lysodeikticus* peptidoglycan is more susceptible to AtlA than homologous peptidoglycan could be due to an unusually high amount of unsubstituted MurNAc residues leading to a low cross-linked molecule therefore quickly solubilized by the enzyme (14). Alternatively, a lower degree of *O*-acetylation of the *M. lysodeikticus* peptidoglycan could explain this difference as *O*-acetylation has been shown to modulate autolysin activity (5, 22).

Determination of AtlA hydrolytic bond specificity. To identify the peptidoglycan bond cleaved by AtlA, we compared the structure of the muropeptides obtained after hydrolysis of *E. faecalis* OG1RF peptidoglycan by the purified AtlA protein and a commercially available muramidase (mutanolysin). After digestion and reduction, the muropeptides were separated by

173 rp-HPLC on a C₁₈ column (Fig. 2A and 2B) and the peaks containing the main monomers,
174 dimers, trimers and tetramers were analyzed by mass spectrometry (MS) (Fig. 2C). The major
175 muropeptides obtained with mutanolysin (peaks 1 to 8) had the same mass as their counterparts
176 obtained after digestion with the purified AtlA protein (peaks 1' to 8'), confirming that AtlA
177 cleaves the glycan moiety of the peptidoglycan. *N*-acetylglucosaminidases and *N*-
178 acetylmuramidases generate muropeptides carrying GlcNAc or MurNAc at the reducing end of
179 the disaccharide, respectively. To discriminate between these two activities, tandem mass
180 spectrometry (MS/MS) was performed on the major muropeptide monomer generated by
181 mutanolysin (Fig. 3A) and AtlA (Fig. 3B). Fragmentation of the ion at *m/z* 1110.6, corresponding
182 to the [M+H]⁺ form of a reduced disaccharide-pentapeptide substituted by an L-alanyl-L-alanyl
183 side chain (DS-penta[AA]), led to different patterns for the two enzymes. For mutanolysin, loss
184 of unreduced GlcNAc gave an ion at *m/z* 907.55 as previously described (24). For AtlA, loss of
185 reduced GlcNAc gave an ion at *m/z* 887.50. Additional loss of alanyl residues from the C-
186 terminus of the pentapeptide or the N-terminus of the side chain gave additional ions
187 characteristic of the muropeptides generated by mutanolysin (Fig. 3A) and AtlA (Fig. 3B),
188 carrying either unreduced or reduced GlcNAc respectively. As expected, ions corresponding to
189 peptides resulting from the loss of both sugars were found in the two fragmentation patterns.
190 These data show that MS/MS is a powerful method for discriminating between muropeptides
191 generated by *N*-acetylmuramidases and those generated by *N*-acetylglucosaminidases and clearly
192 demonstrates that AtlA displays the latter specificity (EC 3.2.1.52). Characterization by other
193 techniques of autolysins related to AtlA indicated that the protein family includes both *N*-
194 acetylmuramidases, such as Mur-2 from *E. hirae* (11), and *N*-acetylglucosaminidases, such as
195 AcmA from *Lactococcus lactis* (21) and LytG from *Bacillus subtilis* (15).

196 **Domain organization of AtlA.** Sequence comparison (data not shown) revealed that the three
197 domains of the AtlA protein are present in different combinations in proteins from various
198 databases, allowing approximate boundaries to be defined as depicted in Fig. 4A. The T/E-rich
199 region is found in *E. faecalis* AtlA homologs (EF0252 and EF1823; www.tigr.org) as well as in
200 *Enterococcus faecium* AtlA homologs (contig 643 and 533; <http://genome.jgi-psf.org>, database
201 released June 2004). No function has been assigned to this low complexity region. The central
202 domain is similar to the catalytic domain of several autolysins from Gram-positive bacteria
203 including *B. subtilis*, *L. lactis*, *E. hirae* (see above), as well as those from *E. faecium*,
204 *Staphylococcus aureus*, *Streptococcus pyogenes* or *Listeria monocytogenes*. Finally, the LysM
205 domain is composed of six LysM modules of approximately 50 amino acids. These modules form
206 $\beta\alpha\beta$ secondary structures separated by intervening sequences of 15-20 residues (3). LysM
207 modules occur most often in cell wall degrading enzymes but are also present in many other
208 bacterial proteins (3). The LysM modules bind to peptidoglycan but the nature of the interaction
209 remains to be characterized.

210 In this study, we have developed two approaches to gain insights into the role of the three
211 domains of AtlA in its enzyme activity. First, fragments of the *atlA* open reading frame were
212 cloned in an *E. coli* expression vector and the corresponding polypeptides were purified. Second,
213 AtlA was partially digested by proteinase K to experimentally probe its domain organization and
214 identify sites sensitive to proteolytic cleavage that might be involved in activation of a putative
215 proenzyme.

216 **Purification of AtlA domains produced in *E. coli*.** The polypeptides corresponding to the
217 different domains of AtlA were produced in *E. coli* and purified by affinity chromatography as
218 described in the Materials and Methods section. Domain II alone, domain III alone and domains

219 I-II were successfully purified to homogeneity (Fig. 4B). As domains II-III were produced at a
220 very low level in *E. coli*, this fragment of AtlA was generated by partial digestion of the mature
221 protein (see below).

222 **Probing of the structural organization of AtlA by limited proteinase K digestion.** The first
223 cleavage by proteinase K generated a protease-resistant core (polypeptide A, Fig. 4C) with an
224 estimated molecular weight of 62 kDa. A polypeptide with a similar apparent molecular weight
225 displaying lytic activity against *M. lysodeikticus* cells was detected in crude extracts of *E. faecalis*
226 (Fig. 4D, lane 1). Since no autolytic activity is detected in crude extracts of the *E. faecalis*
227 OG1RF *atlA* mutant (Fig. 4D, lane 2), these results suggested that AtlA is cleaved *in vivo* in the
228 original host. The N-terminal sequence of the 62 kDa polypeptide obtained *in vitro* was SALSPT,
229 indicating a cleavage between Phe 171 and Ser 172, near the transition between domain I and II
230 as deduced from sequence analysis (Ser 181 – Glu 182; Fig. 4A). The corresponding fragment
231 was purified by size-exclusion chromatography (Fig. 4E) for enzymatic analyses. Further
232 proteolysis events (Fig. 4C) gave rise to polypeptides B (56 kDa) and C (50 kDa). These
233 polypeptides had the same N-terminal sequence, suggesting that they resulted from the sequential
234 loss of one or two LysM modules (ca. 6 kDa) from the C-terminus of the protein.

235 **The central domain of AtlA is catalytically active.** Domain II alone displayed enzymatic
236 activity although it was much less active than AtlA (4.85 ± 0.4 U vs $1,900 \pm 290$ U). This result
237 confirmed that domain II is the catalytic domain of AtlA and indicated that one or both of the N-
238 terminal and the C-terminal domains are required for optimal activity.

239 **The N-terminal T/E-rich domain does not function as a propeptide.** As described above,
240 the zymogram of *E. faecalis* crude extracts indicated that AtlA is cleaved by endogenous
241 proteases (Fig. 4D). To test whether domain I functions as a propeptide, we compared (i) the
242 activity of domains I-II-III with that of domains II-III and (ii) the activity of domains I-II with

243 that of domain II alone. The activity of AtlA was similar to that of domains II-III ($1,900 \pm 290$ U
244 vs $2,830 \pm 420$ U, respectively). Similarly, the activity of domains I+II was similar to that of
245 domain II alone (6.97 ± 0.9 U vs 4.85 ± 0.4 respectively). In agreement with these results, the rate
246 of hydrolysis of *M. lysodeikticus* peptidoglycan by AtlA did not increase upon addition of
247 proteinase K to the reaction mixture (data not shown). Since the addition of exogenous proteases
248 increases the autolysis rate in *E. faecalis* (18), it is likely that another autolysin (different from
249 AtlA) is activated by proteolysis in this bacterium. This putative autolysin could be related to the
250 *E. hirae* Mur-1 enzyme, which is also activated by proteolysis (16). Further experiments are
251 required to identify the role of the T/E-rich region, which may be involved in post-translational
252 modification of AtlA, sub-cellular targeting or interaction with protein(s) modulating its activity.

253 **The LysM domain is critical for AtlA activity.** As expected, domain III (consisting of six
254 LysM modules) displayed no enzymatic activity and was able to bind peptidoglycan *in vitro* (data
255 not shown). The impact of the LysM domain on AtlA activity was tested by comparing (i) the
256 activity of domains I-II-III with that of domains I-II and (ii) the activity of domains II-III with
257 that of domain II alone. Truncation of domain III from the full length protein led to a 270-fold
258 reduction in activity. Similarly, the truncation of domain III from domains II-III led to a 580-fold
259 reduction of activity. Altogether, our results show that cell wall binding is critical for full AtlA
260 activity. Zymogram analyses have been used to investigate the activity of AcmA from *L. lactis*
261 which is made of a catalytic domain fused to a C-terminal LysM domain. Deletion of the LysM
262 modules of AcmA led to an inactive protein indicating that the peptidoglycan-binding domain is
263 also important for the activity of this autolysin (21). The critical role of LysM modules suggests
264 that the activity of autolysins may be controlled at the level of binding of the enzymes to their
265 substrate. The binding onto the cell wall may increase the local concentration of the enzyme or
266 may provide proper positioning of the catalytic domain towards its substrate. Alternatively the

267 LysM domain may be required to induce a proper conformation of the catalytic domain as
268 described for the *Streptococcus pneumoniae* LytA autolysin (7).

269

ACKNOWLEDGMENTS

270 We thank Barbara Murray (University of Texas Medical School, Houston, USA) for providing *E.*
271 *faecalis* OG1RF and OG1RF *atIA* and Jean-Claude Huet (INRA, Jouy en Josas, France) for N-
272 terminal sequencing. Sophie Magnet and Laurent Gutmann are acknowledged for constructive
273 comments on the manuscript.

REFERENCES

- 274
- 275 1. **Amrein, K. E., B. Takacs, M. Stieger, J. Molnos, N. A. Flint, and P. Burn.** 1995.
276 Purification and characterization of recombinant human p50csk protein-tyrosine kinase
277 from an *Escherichia coli* expression system overproducing the bacterial chaperones
278 GroES and GroEL. Proc Natl Acad Sci U S A **92**:1048-52.
- 279 2. **Arbeloa, A., J. E. Hugonnet, A. C. Sentilhes, N. Josseaume, L. Dubost, C.**
280 **Monsempe, D. Blanot, J. P. Brouard, and M. Arthur.** 2004. Synthesis of mosaic
281 peptidoglycan cross-bridges by hybrid peptidoglycan assembly pathways in gram-positive
282 bacteria. J Biol Chem **279**:41546-56.
- 283 3. **Bateman, A., and M. Bycroft.** 2000. The structure of a LysM domain from *E. coli*
284 membrane-bound lytic murein transglycosylase D (MltD). J Mol Biol **299**:1113-9.
- 285 4. **Beliveau, C., C. Potvin, J. Trudel, A. Asselin, and G. Bellemare.** 1991. Cloning,
286 sequencing, and expression in *Escherichia coli* of a *Streptococcus faecalis* autolysin. J
287 Bacteriol **173**:5619-23.
- 288 5. **Bera, A., S. Herbert, A. Jakob, W. Vollmer, and F. Gotz.** 2005. Why are pathogenic
289 staphylococci so lysozyme resistant? The peptidoglycan *O*-acetyltransferase OatA is the
290 major determinant for lysozyme resistance of *Staphylococcus aureus*. Mol Microbiol
291 **55**:778-87.
- 292 6. **Boneca, I. G.** 2005. The role of peptidoglycan in pathogenesis. Curr Opin Microbiol
293 **8**:46-53.
- 294 7. **Briese, T., and R. Hakenbeck.** 1985. Interaction of the pneumococcal amidase with
295 lipoteichoic acid and choline. Eur J Biochem **146**:417-27.

- 296 8. **Cabanes, D., O. Dussurget, P. Dehoux, and P. Cossart.** 2004. Auto, a surface
297 associated autolysin of *Listeria monocytogenes* required for entry into eukaryotic cells
298 and virulence. *Mol Microbiol* **51**:1601-14.
- 299 9. **Chastanet, A., J. Fert, and T. Msadek.** 2003. Comparative genomics reveal novel heat
300 shock regulatory mechanisms in *Staphylococcus aureus* and other Gram-positive bacteria.
301 *Mol Microbiol* **47**:1061-73.
- 302 10. **Da Costa, B., C. Chevalier, C. Henry, J. C. Huet, S. Petit, J. Lepault, H. Boot, and B.**
303 **Delmas.** 2002. The capsid of infectious bursal disease virus contains several small
304 peptides arising from the maturation process of pVP2. *J Virol* **76**:2393-402.
- 305 11. **Dolinger, D. L., L. Daneo-Moore, and G. D. Shockman.** 1989. The second
306 peptidoglycan hydrolase of *Streptococcus faecium* ATCC 9790 covalently binds
307 penicillin. *J Bacteriol* **171**:4355-61.
- 308 12. **Fontana, R., M. Boaretti, A. Grossato, E. A. Tonin, M. M. Lleo, and G. Satta.** 1990.
309 Paradoxical response of *Enterococcus faecalis* to the bactericidal activity of penicillin is
310 associated with reduced activity of one autolysin. *Antimicrob Agents Chemother* **34**:314-
311 20.
- 312 13. **Foster, S. J., D.L. Popham.** 2001. Structure and synthesis of cell wall, spore cortex,
313 teichoic acids, S-layers and capsules, p. 21-41. *In* A. L. Sonenshein, Hoch, J.A. & Losick
314 R. (ed.), *Bacillus subtilis* and its closest relatives: from genes to cells. ASM Press,
315 Washington.
- 316 14. **Ghuysen, J. M., E. Bricas, M. Lache, and M. Leyh-Bouille.** 1968. Structure of the cell
317 walls of *Micrococcus lysodeikticus*. 3. Isolation of a new peptide dimer, *N*-alpha-[L-
318 alanyl-gamma-(alpha-D-glutamylglycine)]-L-lysyl-D-alanyl-*N*-alpha-[L-alanyl-gamma-
319 (alpha-D-glutamylglycine)]-L-lysyl-D-alanine. *Biochemistry* **7**:1450-60.

- 320 15. **Horsburgh, G. J., A. Atrih, M. P. Williamson, and S. J. Foster.** 2003. LytG of *Bacillus*
321 *subtilis* is a novel peptidoglycan hydrolase: the major active glucosaminidase.
322 *Biochemistry* **42**:257-64.
- 323 16. **Kawamura, T., and G. D. Shockman.** 1983. Purification and some properties of the
324 endogenous, autolytic N-acetylmuramoylhydrolase of *Streptococcus faecium*, a bacterial
325 glycoenzyme. *J Biol Chem* **258**:9514-21.
- 326 17. **Milohanic, E., R. Jonquieres, P. Cossart, P. Berche, and J. L. Gaillard.** 2001. The
327 autolysin Ami contributes to the adhesion of *Listeria monocytogenes* to eukaryotic cells
328 via its cell wall anchor. *Mol Microbiol* **39**:1212-24.
- 329 18. **Qin, X., K. V. Singh, Y. Xu, G. M. Weinstock, and B. E. Murray.** 1998. Effect of
330 disruption of a gene encoding an autolysin of *Enterococcus faecalis* OG1RF. *Antimicrob*
331 *Agents Chemother* **42**:2883-8.
- 332 19. **Sahm, D. F., J. Kissinger, M. S. Gilmore, P. R. Murray, R. Mulder, J. Solliday, and**
333 **B. Clarke.** 1989. *In vitro* susceptibility studies of vancomycin-resistant *Enterococcus*
334 *faecalis*. *Antimicrob Agents Chemother* **33**:1588-91.
- 335 20. **Schleifer, K. H., and O. Kandler.** 1972. Peptidoglycan types of bacterial cell walls and
336 their taxonomic implications. *Bacteriol Rev* **36**:407-77.
- 337 21. **Steen, A., G. Buist, G. J. Horsburgh, G. Venema, O. P. Kuipers, S. J. Foster, and J.**
338 **Kok.** 2005. AcmA of *Lactococcus lactis* is an N-acetylglucosaminidase with an optimal
339 number of LysM domains for proper functioning. *Febs J* **272**:2854-68.
- 340 22. **Strating, H., and A. J. Clarke.** 2001. Differentiation of bacterial autolysins by
341 zymogram analysis. *Anal Biochem* **291**:149-54.
- 342 23. **Weidel, W., and H. Pelzer.** 1964. Bagshaped macromolecules - a new outlook on
343 bacterial cell walls. *Adv Enzymol Relat Areas Mol Biol* **26**:193-232.

- 344 24. **Xu, N., Z. H. Huang, B. L. de Jonge, and D. A. Gage.** 1997. Structural characterization
345 of peptidoglycan muropeptides by matrix-assisted laser desorption ionization mass
346 spectrometry and postsource decay analysis. *Anal Biochem* **248**:7-14.

347

FIGURE LEGENDS

348 **Figure 1. Purification of AtlA and determination of the optimal pH for activity.** (A)
349 Purification of AtlA: lane 1, Crude extract of BL21 DE3 (pREP4GroESL) transformed with
350 pET2818 after IPTG induction (15 µg of protein); lane 2, crude extract of BL21 DE3
351 (pREP4GroESL) transformed with pML118 after IPTG induction (15 µg); lane 3, protein fraction
352 eluting from metal affinity chromatography with 100 mM imidazole (5 µg); lane 4, protein
353 fraction eluted with 100-200 mM NaCl from the anion-exchange column (4 µg). (B) pH activity
354 profile of AtlA. Enzymatic activity was assayed on *M. lysodeikticus* cell walls at 37°C.

355

356 **Figure 2. Digestion of *E. faecalis* peptidoglycan by mutanolysin and AtlA.** Rp-HPLC
357 muropeptide profiles of OG1RF peptidoglycan digested by mutanolysin (A) or AtlA (B). The
358 mass and predicted structures for peaks 1 to 8 and 1' to 8' are described in (C).

359

360 **Figure 3. Determination of AtlA cleavage specificity by MS/MS.** The major muropeptide
361 monomers generated by mutanolysin (peak 2) and AtlA (peak 2') were analyzed by MS/MS
362 yielding fragmentation patterns (A) and (B), respectively. The m/z values of the most informative
363 ions are boxed and the inferred structures are indicated with a one-letter code: M, MurNAc; M^R,
364 reduced MurNAc; G, GlcNAc; G^R, reduced GlcNAc; A, L-Ala or D-Ala; Lac, D-lactate; K, L-
365 Lys; Q, D-*iso*-Gln.

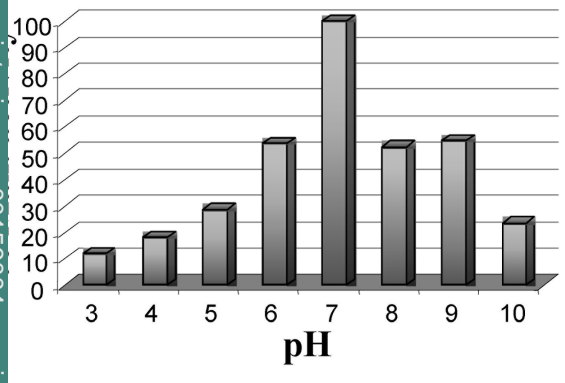
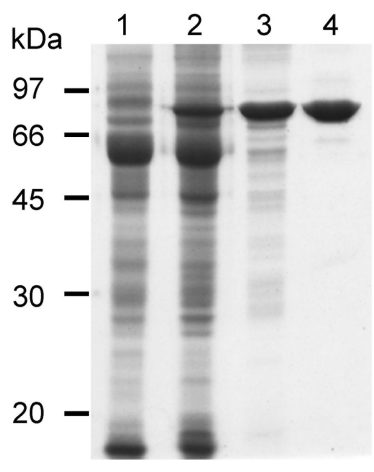
366

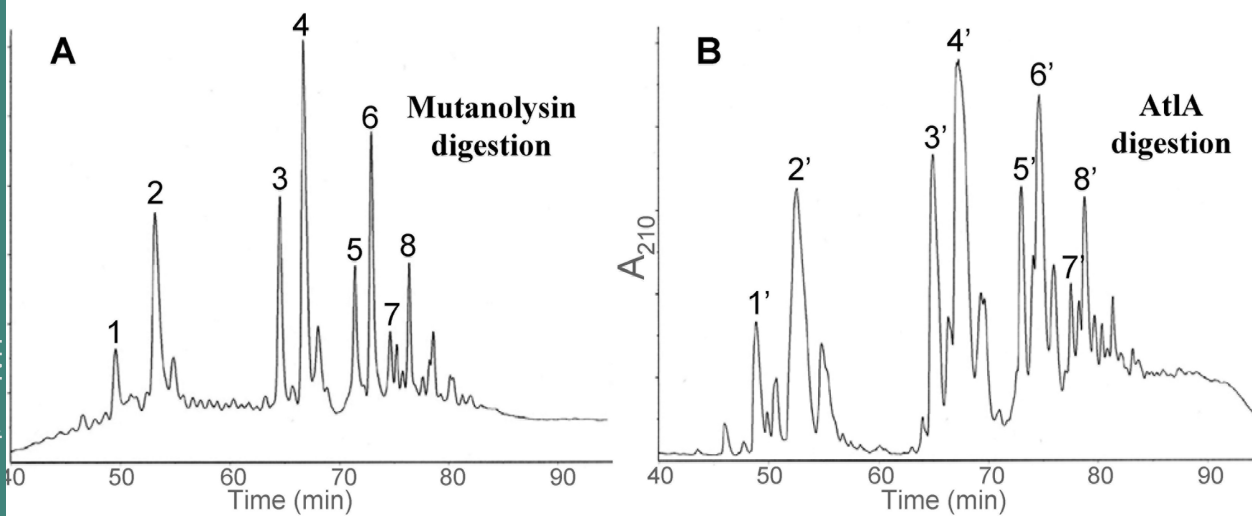
367 **Figure 4. Domain organization of AtlA.** (A) Domain organization of AtlA deduced from
368 sequence analysis. SP, signal peptide; T/E-rich, threonine- and glutamic acid-rich region
369 (domain I); Catalytic, catalytic domain (domain II); LysM, LysM domain (domain III). (B)
370 Purification of AtlA and its derivatives overexpressed in *E. coli*. Lane 1, domains I-II (2 µg); lane

371 2, domain II alone (2 μ g); lane 3, domain III alone (4 μ g). (C) Limited digestion of AtIA by
372 proteinase K. Full length AtIA (10 μ g, lane 1) was digested with proteinase K and aliquots were
373 withdrawn after 1 min (lane 2), 5 min (lane 3) or 10 min (lane 4). The three polypeptides A, B C
374 (indicated by an arrow) were subjected to N-terminal sequencing. (D) Zymogram showing cell
375 wall lytic activity of AtIA. Proteins were separated by SDS-PAGE in a gel containing 0,2% of
376 autoclaved *M. lysodeikticus* cells, renatured *in situ*, and incubated at 37°C. Lane 1, crude extract
377 of OG1RF (20 μ g); lane 2, crude extract of OG1RF *atIA* (20 μ g) (18). (E) Purification of
378 truncated AtIA lacking the N-terminal domain. The full length AtIA was subjected to limited
379 digestion by proteinase K. The digestion products were loaded on a size-exclusion column to
380 separate undigested AtIA (domains I-II-III) from AtIA devoid of its N-terminal region (domains
381 II-III). Inset: lane 1, undigested AtIA; lane 2, partial digest; lane 3, purified peak a; lane 4,
382 purified peak b. The unexpected high retention time of domains II-III could result from non
383 specific interaction of this polypeptide with the sephadex matrix of the column.

Table 1. Bacterial strains, plasmids and oligonucleotides.

Strains/plasmids/oligonucleotides	Relevant properties	Source
Strains		
<i>Enterococcus faecalis</i>		
V583	Sequenced strain (clinical isolate)	(18)
OG1RF		(17)
OG1RF <i>atIA</i>		(17)
<i>Micrococcus lysodeikticus</i>		
ATCC4698		Pasteur Institute
<i>Escherichia coli</i>		
BL21(DE3) pREP4GroESL	Expression strain	(1)
XL1-blue	Cloning strain	Stratagene
Plasmids		
pET28/16	pET28a derivative	(7)
pET2818	pET28/16 variant for C-terminal Histidine-tag fusion	Lab stock
pML118	pET2818 carrying an <i>AtIA</i> fragment encoding residues 54 to 737	This work
pML318	pET2818 carrying an <i>AtIA</i> fragment encoding residues 54 to 335	This work
pML418	pET2818 carrying an <i>AtIA</i> fragment encoding residues 182 to 335	This work
pML518	pET2818 carrying an <i>AtIA</i> fragment encoding residues 335 to 737	This work
Oligonucleotides		
	Sequence (5'→3')	
EF0799-1	ttccatggggacagaagagcagccaacaaatgc	
EF0799-2	ttggatcagaagatggtgtatcatattg	
EF0799-3	ttccatggggtcagaatttattgccgagttagc	
EF0799-4	ttggatccaccaacttttaaagttgaccaa	
EF0799-5	aaacctgggaacgaacacgtactatactgtaaaatc	

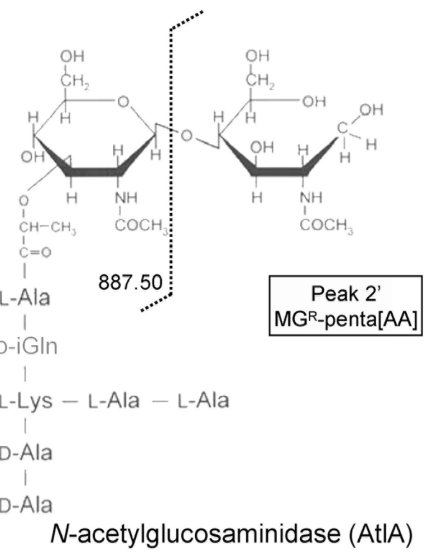
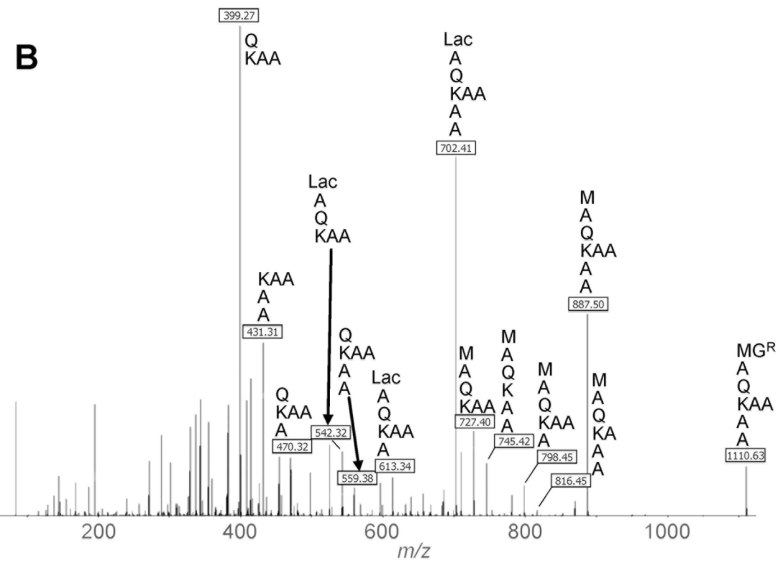
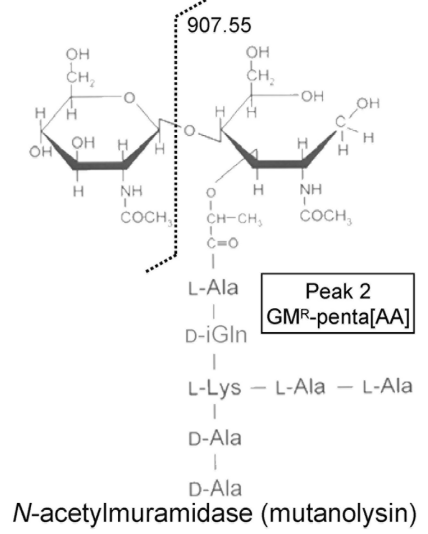
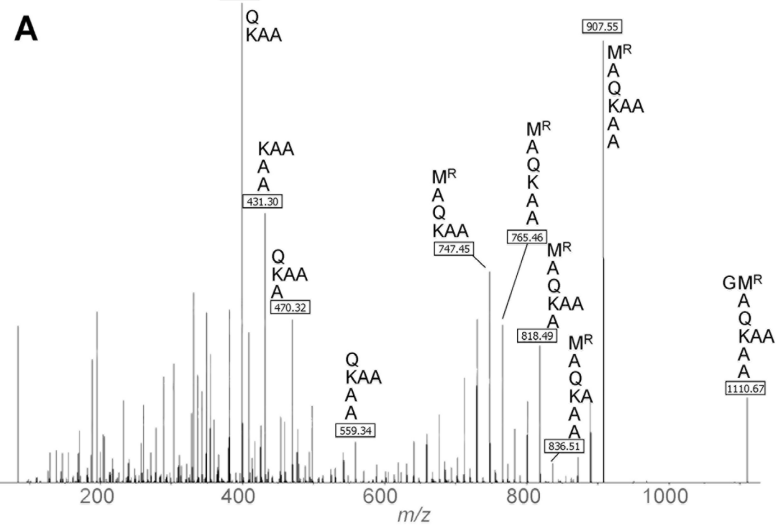


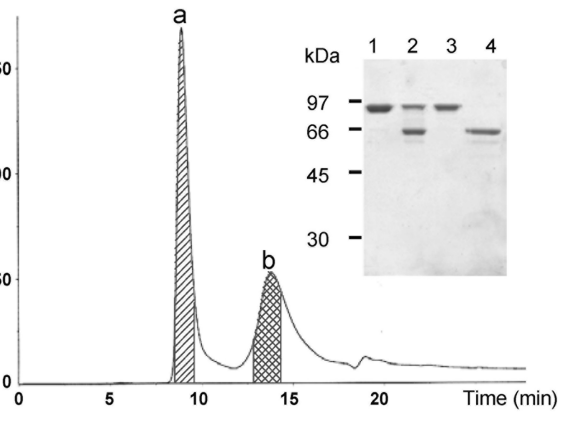
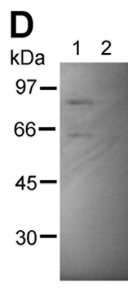
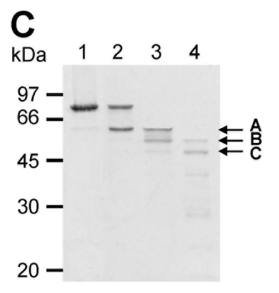
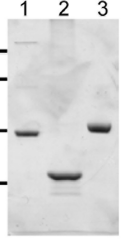
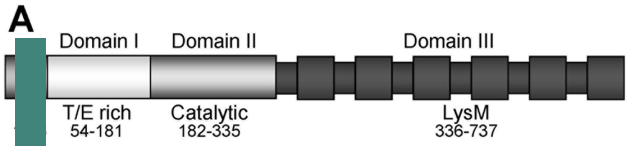


C

Major mucopeptide ^a	Monoisotopic mass		
	Calculated	Observed (peak number)	
		mutanolysin	AtIA
Monomers			
DS tri[AA]	967.47	967.47 (1)	967.46 (1')
DS penta[AA]	1,109.55	1,109.67 (2)	1,109.49 (2')
Dimers			
DS tri[AA]-DS tetra[AA]	1,987.97	1,987.93 (3)	1,987.94 (3')
DS penta[AA]-DS tetra[AA]	2,130.04	2,130.03 (4)	2,130.01 (4')
Trimers			
DS tri[AA]-(DS tetra[AA]) ₂	3,008.47	3,008.43 (5)	3,008.49 (5')
DS penta[AA]-(DS tetra[AA]) ₂	3,150.54	3,150.51 (6)	3,150.48 (6')
Tetramers			
DS tri[AA]-(DS tetra[AA]) ₃	4,028.96	4,028.93 (7)	4,028.96 (7')
DS penta[AA]-(DS tetra[AA]) ₃	4,171.04	4,171.00 (8)	4,171.08 (8')

^a Mucopeptide contained reduced disaccharides (DS). The pentapeptide (penta), tetrapeptide (tetra), and tripeptide (tri) stems were substituted by an L-alanyl-L-alanyl side chain [AA].





HAL author manuscript inserm-00156004, version 1